PROCEEDINGS, INDONESIAN PETROLEUM ASSOCIATION
Thirty-First Annual Convention and Exhibition, May 2007

INFLUENCE OF POROSITY AND FACIES OF BATURAJA CARBONATE TO THE SEISMIC WAVE VELOCITY: CASE STUDY OF TAMBUN FIELD WEST JAVA

Jarot Setyowiyoto*
Bagus Endar B. Nurhandoko**
Ariffin Samsuri***
Bambang Widjanarko****
Thurisina**

ABSTRACT

The early Miocene Baturaja Formation is one of the most prolific reservoirs in Tambun Field, West Java. The hydrocarbon mostly comes from the Upper Baturaja Formation reservoirs. These carbonate rocks show some complex porosity, lithology and facies.

This study includes detail relationship among reservoir petrophysics , elastic wave parameters, effect of water saturation, pore type and facies of Baturaja carbonate rock to the seismic wave parameter, such as compressional and shear wave velocity.

Many data were collected and studies carried out to obtain detailed relationships between seismic attributes and petrophysical parameters of the Baturaja carbonate, such as: petrographic analysis, SEM image, detail core description, well logging data analysis and laboratory experimental of seismic wave velocities measurements in variation of overburden pressure, pore pressure and temperature. Some seismic wave parameters were simulated as close as possible to the reservoirs condition.

The result shows that the seismic wave velocity in the Baturaja carbonate has wide value range, i.e: compressional wave velocity (Vp) ranges from 3300 to 4000 m/s and shear-wave velocity (Vs) from 1500 to 2000 m/s.

Based on petrophysical data and seismic wave measurement, the total porosity is not the only main factor controlling elastic wave parameters, as a matter of fact, the pore type plays also important role. A plot of porosity versus velocity displays an inverse trend encountered in the zone B and D, for zone A and C the diagram are slightly scatter. It is shown also that there is strong relationship between seismic wave velocity and lithology facies, therefore this result proves that seismic waves can be applied to facies determination in carbonates of Baturaja formation.

* Gadjah Mada University
** Institute of Technology Bandung
*** Universiti Teknologi Malaysia
**** Pertamina-Jawa Region

INTRODUCTION

The Carbonates result mainly from biochemical and biological processes in warm shallow marine and lacustrine environments and prone to rapid and pervasive diagenetic alterations that change the mineralogy and pore type within carbonate rocks. Most porosity in carbonate rocks is diagenetic in origin, and as result it has some complexity in porosity, which will be controlled by the original facies type and later diagenetic processes (Tucker et al., 2001). Such diagenetic processes continuously modify the pore structure to create or destroy porosity. Cementation diagenetic processes for instance are prone to reduce porosity while dissolution will enlarge porosity. All these modifications will effect seismic wave velocity such as compressional wave velocity (Vp) and shear wave velocity (Vs).

Tambun Field is located in the West Java Province and the hydrocarbons are reservoired mainly in Baturaja Formation (BRF). This formation consists of bio-clastic carbonates rock, carbonate reef and overlies conformably on the top of Talang Akar Formation. BRF was deposited in the early Miocene, showing development of fully open marine conditions.

The objective of this study includes detail relationship among reservoir petrophysics, elastic wave parameters, effect of water saturation, pore type and facies of Baturaja carbonate rock to the

seismic wave parameter, such as compressional and shear wave velocity.

Geological Framework (structure and stratigraphy)

The Northwest Java Basin Province lies mainly in the waters of Indonesia and includes some onshore areas of Java (Figure 1). The province includes the basins of Sunda and Asri in the offshore southeastern Sumatra region and extends eastward across the Java Sea to the Ardjuna Basin region and Jatibarang Basin. Tambun field lies in the onshore of the province which is currently positioned in back arc setting. The Northwest Java depression is asymmetrical, with its deepest Arjuna Basin lies at the foot of the Arjuna Plateau, separated by a major N-S trending fault. The basin opens south-ward into the onshore Ciputat, Pasir Putih and Jatibarang Basins (Bishop, 2000).

General stratigraphy of this onshore basin, from the oldest to the youngest, are : Jatibarang Formation, Talangakar Formation, Baturaja Formation, Cibulakan Formation, Parigi Formation and Cisubuh Formation (Figure 2) (Gordon, 1985; Wicaksono et al., 1992; Kalan et al., 1994; Pertamina, 1996; vide Bishop, 2000).

1. Jatibarang Formation

The Eocene to Oligocene Jatibarang Formation, unconformably, underlain by the pre-Tertiary metamorphic basement rock. Jatibarang Formation consists of andesite lavas at the base and dacite basaltic lavas interbedded with volcanic rocks such as tuff, amalgamated tuff and andesitic/basaltic tuff and volcaniclastic sands in the upper parts. This formation was unconformably overlain by Talang Akar Formation.

2. Talang Akar Formation

The Talang Akar Formation of Oligocene to early Miocene age overlies the the Jatibarang Formation and basement rocks. The formation is characterized as synrift to late rift continental style deposition. The lower part represents continental deposition (fluvial system siliciclastic rock) and the upper part represents an increasing marine transgression and upward lack of the volcanic materials influence.

3. Baturaja Formation

The early Miocene Baturaja Formation (BRF) consists of bio-clastic carbonate rocks, carbonate reef and overlies conformably on the top of Talang Akar Formation. BRF was deposited in the open marine environment.

4. Cibulakan Formation

This formation is characterized by clastic-carbonate rocks. Carbonates reef developed in the middle of this formation, named as "Mean Carbonates". The early-middle Miocene of Cibulakan Formation is determined as "P" layer and has contact with Parigi Formation carbonates in the top. Transition zone between Cibulakan Formation and Parigi Formation is subdivided into units from "O" unit to "D" unit. Noted there are some horizons in this formation such as Zone 14 and Zone 15 which is served as a marker.

5. Parigi Formation

The late Miocene Parigi Formation developed on structurally stable shallow marine platforms as bioherms associated with paleohighs but not necessarily basement highs. This formation, formed in the low-energy environment, produce fine grained rocks, shaly lime mud and packstone - wackestone facies. The lower part of this formation is characterized by gradual changes of mixed facies of clastic carbonates of the Cibulakan Formation. Top of Parigi Formation is overlain by Cisubuh Formation which could be seen clearly as clastic-carbonates and carbonaceous shale.

6. Cisubuh Formation

The Pliocene Cisubuh Formation is the youngest formation in the basin, dominated by carbonaceous shale and thin bed sandstone. Cisubuh shale forms the main seal for Parigi carbonate reservoirs. Upward, the thicker sand was developed in this formation. Glauconite and thin coal seams are often found in the upper part of this formation. Cisubuh Formation overlies conformably Parigi Formation.

Method and Data Collection

Logging data from Well # JS - 08, 10 and 14 used in this study comprises of Spotaneous Potential Log (SP), Micro Spherical Focused Log (MSFL), Laterolog Shallow (LLS), Laterolog Deep (LLD), Gamma Ray Log (GR), Formation Density Log (FDL), Compensated Neutron Log (CNL) and Sonic log. Petrophysical properties analysis of the well logging data has been conducted to obtain the value of porosity, permeability and water saturation.

Twenty one carbonate core samples have been analysed for detailed core description, petrophysics, petrography, Scanning Electron Microscope (SEM) and X-Ray Diffraction (X-RD). Twelve cylindrical core-plug samples from those were analyzed in the Wave Inversion and Subsurface Fluid Imaging Research Laboratory to obtain the value of compressional wave velocity (Vp) and shear wave velocity (Vs) in variation of overburden pressure, pore pressure and also temperature. Some acoustic wave parameters were simulated as close as possible to the reservoirs condition. The samples were cleaned in methanol and dried in a vacuum oven at 85°C for period of twenty-four hours and than saturated by brine/formation water with NaCl of 16,271.67 mg/l. The acoustic velocity measurement on the carbonate samples have been performed under brine saturated conditions at frequencies of about 10 Hz, the overburden pressure range from 500-5000 psig, the pore pressure range from 500-5000 psig, and temperature range from 27-70°C. These procedures were run in Wave Inversion and Subsurface Fluid Imaging Research Laboratory, Institute Technology of Bandung.

Petrographic analysis was undertaken on all the cores which had been impregnated with araldite resin to maintain the existing natural porosity and staining for carbonate minerals with solution of Alizarin Red-S. The carbonate coloration given by staining is as follows: pink color for calcite, bluish pink to blue for ferroan calcite, dark blue to greenish blue for ferroan dolomite and unstained for dolomite.

In order to obtain an understanding of diagenetic fabrics, particularly clay and micrite, and their roles with respect to reservoir quality, SEM-EDX analysis was also conducted. The samples were cleaned using organic solvents and ultrasound treatment, then were broken to create fresh surface and mounted on 10 mm Cu-stub. They were air brushed free of dust and other contaminants, placed under vacuum overnight to remove most remaining volatile, and electrostatically coated with both carbon and gold alloy. XRD analyses were prepared for all samples to quantitatively determine whole rock and clay mineralogy in terms of weight percent of the whole rock. Clay mineral analysis involved ultrasonic disaggregation and centrifugation to isolate the clay fraction, followed by the preparation of oriented clay mounts that were run in untreated, heated (360°C) and glycolated states. The petrography, porosity and permeability measurement, SEM-EDX and X-RD were performed in the Research and Development Centre for Oil and Gas Technology (Lemigas) Laboratory Jakarta.

Carbonate Facies Analysis

Carbonate facies has been determined base on characteristic of lithology, texture, sedimentary structure, composition and fossil content. Detail core description of the depth 2072.00m - 2078.79m supported by integrated petrography, Scanning Electron Microscopy (SEM), Energy Dispersive X-ray (EDX) and X-Ray Diffraction (X-RD) analysis have identified four facies units i.e.:

Facies 1: Large Forams Grainstone Facies

The facies in general is white in colour or light grey when wet due to minor clay mixtures, common grainstone facies alternation with floatstone and locally packstone.

Parallel bedding sedimentary structures were observed in the depth interval of 2072.00m-

2072.26m (Figure 3.A) and cross bedding structures were encountered in the depth interval of 2072.26m-2072.48m (Figure 3.B). It is composed mainly of skeletal grains such as larger benthic foraminifera (Figure 4.A), encrusting and fragmented red algae (Figure 4.B), echinoids and bryozoans. Relics of horizontal burrows are occasionally present.

Petrographic analysis reveals that the grain size range from 0.52mm – 1.8mm and grain contact is dominantly point type. The skeletal framework grains within the samples are composed mainly larger forams (23%-24%) and red algae (14%-16%) and associated with minor amount of echinoid (7%-8%), bryozoans (3%-4.5%), brachiopods (1%-2.2%), small benthonic forams (0.75%-2%), planktonic forams (0.50%) and indeterminate bioclast (2%-2.5%). The detrital grains are also present in trace to minor proportion as monocrystalline quartz (0.50%), carbonaceous materials (2%-3%) and glauconite (0.50%).

Secondary minerals, produced by replacement of grain, matrix and carbonaceous materials, are sparry calcite, microspar, blocky calcite, pyrite, dolomite and anhydrite. Sparry calcite (2%-3%), microspar (1%-2%), and blocky calcite (1%) occur in minor quantities by volume as a result of skeletal grains replacement. Pyrite present in a minor proportion (1%) and formed by replacement of carbonaceous materials. Rhombic dolomite is present in the

samples (4%-6%) produced by replacement of grains, calcite cement and matrix (observed along the stylolite surface trend).

The cementing agents identified within the limestones are calcite, pyrite, quartz and glauconite. Moderately contents of calcite cement are presented in the samples (12%-16%) as pore filling of intergranular and intragranular pore types. Minor proportion of monocrystalline overgrowth of calcite cement is also visible as encrusting on echinoid grains. Both pyrite (2-3.5%) and glauconite (3%-5%) occur as pore filling cement of intragranular pore type. The silica cement (0.75%-1%) generally occurs as quartz filling secondary dissolution pore type. SEM analysis showing vuggy and intragranular pores is cemented by calcite and dolomite causing porosity reduction (Figure 5). EDX analysis (Figure 6) showing that authigenic clay found as illite developed within microporosity. XRD analysis reveals that the samples are mainly composed of calcite (87%-90%) and dolomite (8%-10%) with other minerals consists of quartz (1%) and pyrite (1%-2%).

Facies 2: Large Foram Packstone to Grainstone Facies

The facies in general is light grey or grey when wet due to minor clay mixtures, common grainstone alternation with packstone facies. Cross bedding sedimentary structures were observed in this depth interval (Figure 7). The grains size range 0.22 mm - 3.75 mm, grain to grain contact is point type, moderately sorted and mostly abraded (rounded). The carbonate rock contains commonly large forams (C-I, 5-6; C-G, 2-4; K-L, 8-9: Figure 8-A) and less of red algae (F-G, 8-9; J-M, 6; A-B, 4-5: Figure 8-A), echinoderms (H-I,1-3; H-I, 4-6; G-I, 7-9: Figure 8-B), small benthonic forams (I,3: Figure 8-A), planktonic forams, bryozoan (I-L, 3-5: Figure 8-A) and indeterminate bioclasts. Intergranular pore is
dominant, mostly filled by mosaic calcite cement type. Monocrystal syntaxial overgrowth on some echinoderms grains (G, 1-3; F, 7-8; B, 6-7; C-D, 6-8: Figure 8-B).

Diagenetic processes include micritization of grains, precipitation of minor pyrite and glauconite that fill intragranular voids and styllolite. Moderate calcite fill intergranular and intragranular pores and minor quartz fill secondary dissolution pore. Rhombic and sucrose dolomite formed as a result of calcite grain replacement.

Facies 3 : Red Algal Packstone to Floatstone Facies.

The facies generally is grey in colour or dark grey when wet due to clay mixtures. Minor discontinous thin laminae of detrital clay and carbonaceous materials are present in this facies (Figure 9). The grain size ranges 0.3 mm - 3.75 mm, mostly abraded. Grain to grain contact is dominated by floating type and some of them are point type. The composition is predominantly red algae (D-I, 6-7; A-C, 6-9: Figure 10-A) and larger forams (A-F, 3-4; C-I, 4-5: Figure 10-A). Other grain constituents are minor amount of echinoderms, brachiopods, indeterminate bioclasts and trace of small benthonic and planktonic forams, coral debris, and milliolids. The porosity type is predominantly mouldic and intergranular pores which are mostly filled by mosaic equant calcite cement and minor of pendant calcite cement type (C-D, 6; C-D, 4; D-E, 8: Figure 10-B).

The diagenetic processes occurred in this facies are slight micritisation of grains, precipitation of pyrite and glauconite that fill mouldic and intragranular pore, calcite filling intergranular and intragranular pore, replacement of grains by rhombic dolomite and calcite spar (M, 5; K,8: Figure 10-A), and finally dissolution processes.

Facies 4: Red Algal Floatstone to Grainstone

The facies generally is grey in colour or dark grey when wet due to clay mixtures. Minor discontinous thin laminae of detrital clay and carbonaceous materials are present in this facies (Figure 11).

The grain size ranges 0.37 mm – 5.25 mm, poorly sorted and mostly abraded. Grain to grain contact is dominated by floating type and some of them is point type The composition is predominantly red algae (M,6;C-D,2: Figure 12-A) and larger forams (E-I,5-6;A,3-6;E-G,7: Figure 12-A) and minor amount of echinoderms, brachiopods, indeterminate bioclasts, litho clasts, coral debris, small benthonic and planktonic forams. Blocky calcite (J-M, 7-9: Figure 12-B) and rhombic dolomite (E-F,4-5;G,1;G-H,6: Figure 12-B) are also visible as grains replacement product.

The diagenetic processes occurred in this facies are slightly micritisation of grains, precipitation of pyrite, glauconite filling in the intragranular pore, calcite filling in the intergranular and intragranular pores, replacement of grains by minor amount of calcite

spar, blocky calcite, microspar and rhombic dolomite. The other diagenetic process are stylollitisation and dissolution process.

Interpretation of Depositional Environment

Based on texture, sedimentary structure and composition observed in this carbonate facies, it was suggested that deposition has taken place under a high energy, shallow carbonate platform (Tucker et al., 2001). Variable minor amount of clay mixture occasionally present within this carbonate rock indicated that the platform is attached to the landmass.

The influence of porosity and facies on velocity

Velocity is strongly dependent on the rock-porosity (Wang and Nur, 1992; Rafavich et al., 1984). A plot of porosity versus compressional wave velocity (Vp) generally displays a clear inverse trend; an increase in porosity produces a decrease in velocity (Schoon, 1996; Eberli et al., 2003; Samsuri et al., 2004). In this study the measured values, however, display a slightly scatter and can be grouped into 4 zones (Figure 13). Each zone has some characteristics in lithology facies, pore type and also velocity values. Zone A is Large Forams Grainstone Facies, dominated by vuggy and intragranular porosity with porosity values range from 18% to 23%, this zone can have velocities between 4100 m/s and 4300 m/s. Zone B is Large Foram Packstone to Grainstone Facies, this rock with intergranular porosity between 19% and 29% can have velocities values range from 3840 m/s to 3900 m/s. Zone C is Red Algal Packstone to Floatstone Facies, dominated by mouldic and intergranular porosity range from 23% to 33% with velocity values of 3990 m/s to 4040 m/s. Zone D is Red Algal Floatstone to Grainstone Facies, 15%-27% intergranular porosity, and can have velocities values range from 3910 m/s to 3960 m/s.

Those values slightly scatter around this inverse correlation in velocity-porosity diagram. Velocity can be different at equal porosity in particular at medium porosity. For examples, carbonate rock with porosities of 21% can have velocities between 3840 m/s and 4300 m/s. This could be caused by the different pore type. Likewise, porosity can vary widely at any given velocity. For examples in the zone B, large foram packstone to grainstone facies with a Vp of 3850 m/s can have any porosities anywhere between 19% and 28%. Cross plot of gamma ray versus compressional wave velocity (Vp) for zone B and D shows that increasing of gamma ray resulting in increasing of velocity, for zone A and C the diagram are slightly scatter (Figure 14).

The influence of pressure and temperature on velocity

Velocity is strongly influenced by temperature (Mubarak & Somerton, 1991). Toyasa et al. (vide Sheriff, 1992) noticed large velocity decrease with increasing temperature in core of heavy oil and tars sands. We conducted a series of laboratory investigation on cores of carbonate rock. Compressional (Vp) and shear wave velocities (Vs) were measured in brine saturated carbonate rock in variation of overburden pressure, pore pressure and also temperature.

Figure 15 shows that both Vp and Vs were measured in a brine saturated rock, temperature 28.73 °C, pore pressure (PP) = 0 and influenced by variation of overburden (OB) pressure. In this experiments Vp increase range from 3400 m/s to 3700 m/s, Vs also increase slowly range from 1650 m/s to 1950 m/s when overburden pressure increase from 50 Bar to 475 Bar. The overburden pressure causes compaction, porosity reduction and increasing in velocity. This performance is slightly changed when temperature increase from 28.73 °C to 62.07 °C, generally both Vp and Vs value become lower. The Vp increase range from 3200 m/s to 3600 m/s and Vs values range from 1550 m/s to 1900 m/s (Figure 16).

Other experiment both Vp and Vs were measured in a brine saturated rock, temperature 28.73 °C, overburden (OB) pressure = 0 and influenced by variation of pore pressure (PP). Figure 17 shows that when pore pressure increase from 50 Bar to 400 Bar Vp decrease range from 4010 m/s to 3700 m/s, Vs also decrease slowly range from 2000 m/s to 1950 m/s. This performance is changed when temperature increase from 28.73 °C to 62.07 °C, generally both Vp and Vs value become lower. The Vp decrease range from 4000 m/s to 3600 m/s and Vs values slightly decrease from 1950 m/s to 1900 m/s (Figure 18).

CONCLUSION

Porosity is the main controlling factor in determining sonic velocity in carbonate rocks. Pore type developed in facies is the second controlling factor in determining sonic velocity. Velocity differences at equal porosity could be caused by the

different pore type. Vuggy / moldic pore types of rocks are formed by dissolution of grain, precipitation of cement that form a stiff frame, which provides rigidity to the rock and as a result, this pore type have a high velocity. In contrast, intergranular / intercrystalline porosity type which is caused by fabric destructive dolomitization produces low rigidity and low porosity. Velocity is also strong influenced by pressure and temperature. Increasing overburden pressure will result increasing of velocity, on the other hand increasing of pore pressure produce decreasing of velocity and increasing temperature will result decreasing of velocity.

ACKNOWLEDGMENT

We wish to thank Pertamina for their permission to publish these data and Wave Inversion and Subsurface Fluid Imaging Research Laboratory, Institute Technology of Bandung for seiscore analysis and we also extend our thanks to IRPA Malaysia.

REFERENCE

Bishop, M.G., 2000, Petroleum Systems Of The Northwest Java Province, Java And Offshore Southeast Sumatra, Indonesia, U. S. Geological Survey, Colorado.

Eberli, G.P., Baechile, G.T., Anselmetti, F.S., and Incze, M.L., 2003, Factors Controlling Elastic Properties in Carbonate Sediments and Raocks, The Leading Edge 654-660.

Mubarak, S.A., and Somerton, W.H., 1971, The Effect of Temperature and Pressure on Wave Velocities in Porous Rock, Fall Meeting Alternate, SPE 3571.

Rafavich, F., Kendall, C. H., Todd, T.P., 1984, The Relationship between Acoustic Properties and the Petrographic Character of Carbonate Rocks, Geophysics, Vol 45.

Samsuri, A., Herianto, and Setyowiyoto, J., 2004, Petrophysics Study of Sandstone Core to the Accuracy of Ultrasonic Pulsa Velocity, SOMChe, Universiti Teknologi Petronas, Malaysia.

Schoon, J.C., 1996, Physical Properties of Rocks – Fundamentals and Principles of Petrophysics, Sesismic Exploration Vol. IV, Elsevier Science Ltd.

Sheriff, R.E., 1992, Reservoir Geophysics, Society of Exploration Geophysicist, USA.

Tucker, M.E., Wright, V.P., and Dickson, J.A.D., 2001, Carbonate Sedimentology, Blackwell Science, UK.

Wang, Z., and Nur, A., 1992, Aspects of Rockphysics in Seismic Reservoir Surveillance, Reservoir Geophysics, Edited by Robert E. Sheriff, SEG, Tulsa, Oklahoma.

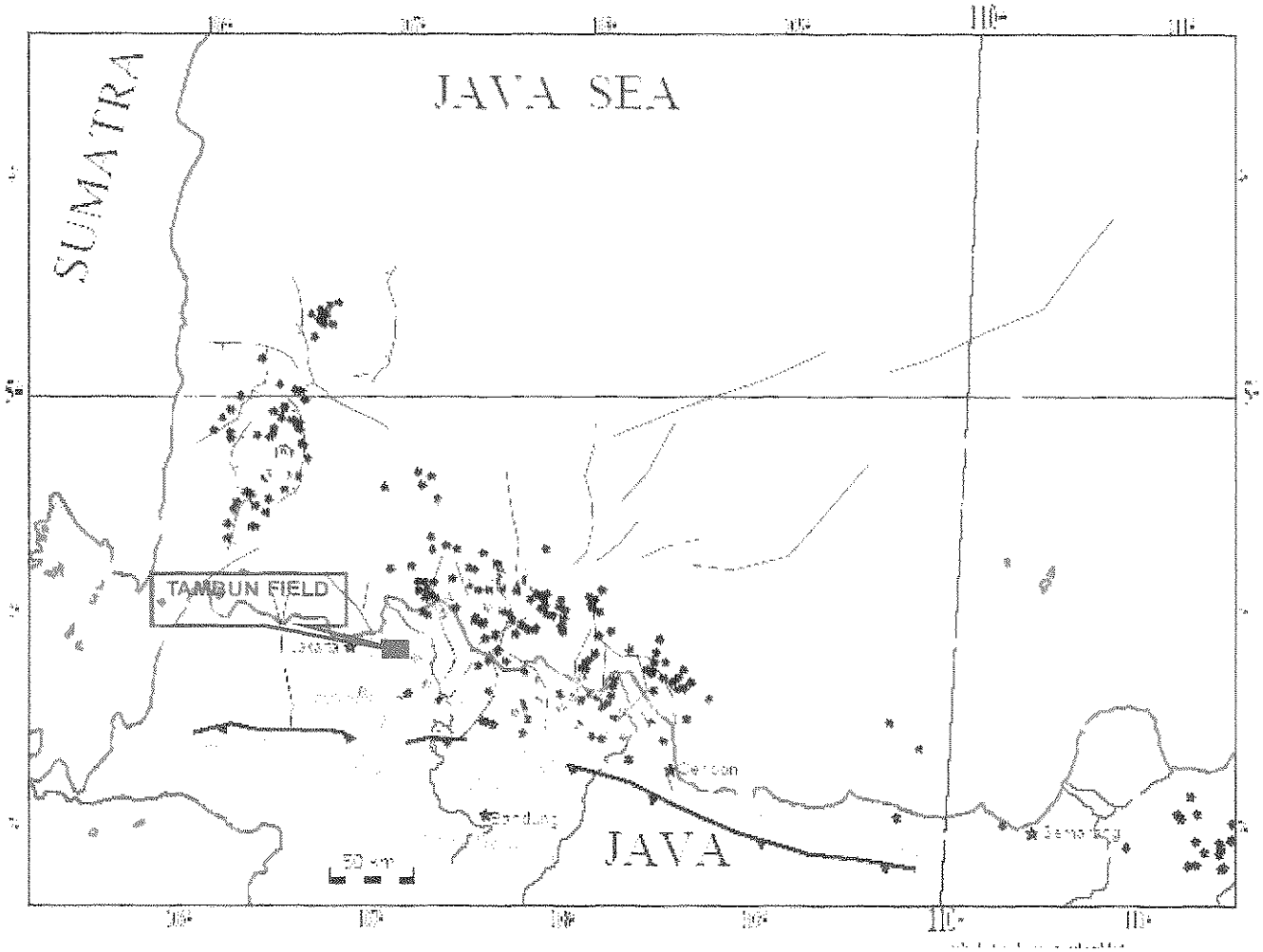

Figure 1 - Northwest Java Basin Province. The Province includes the basins of Sunda and Asri in the offshore southeastern Sumatra region and extends eastward across the Java Sea to the Ardjuna Basin region and Jatibarang Basin. Tambun field lies in the onshore of the province.

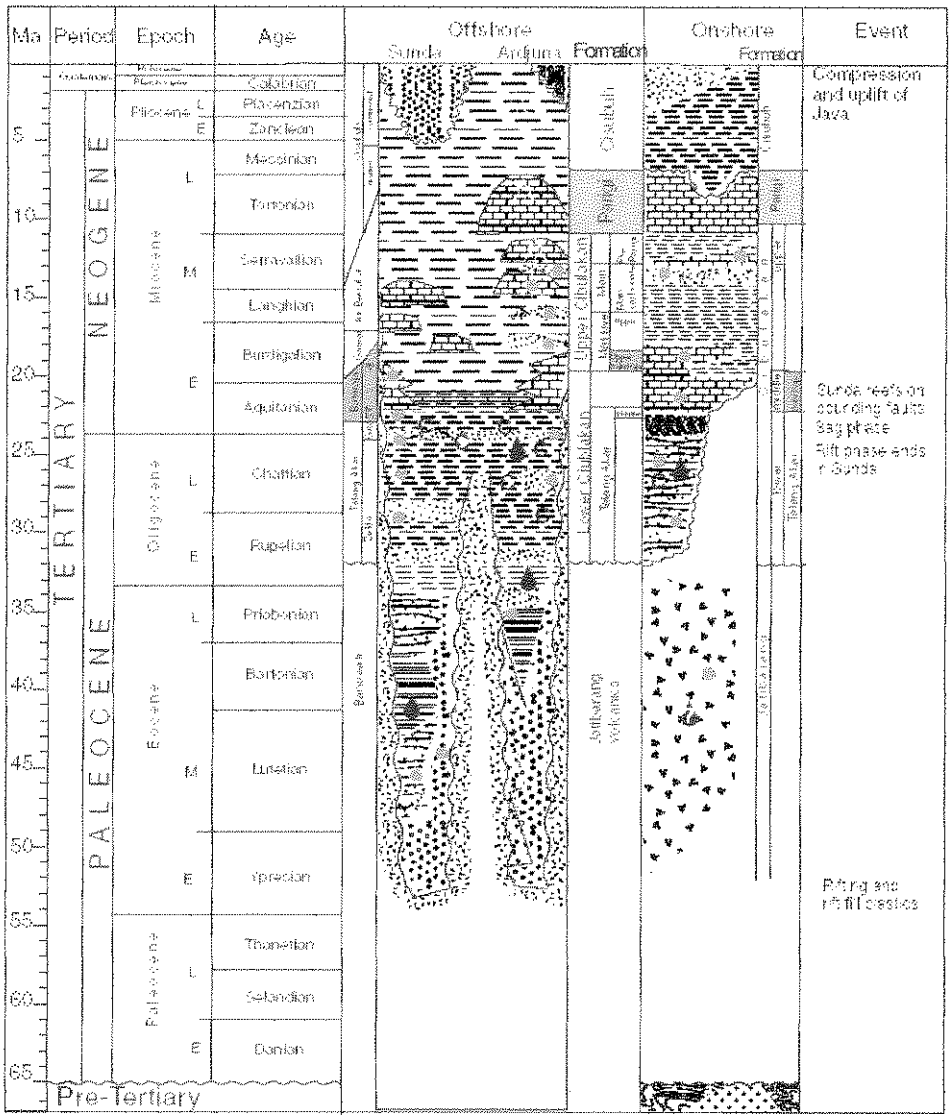

Figure 2 - Generalized stratigraphic columns of the Northwest Java Basin Province, include offshore and onshore basins.

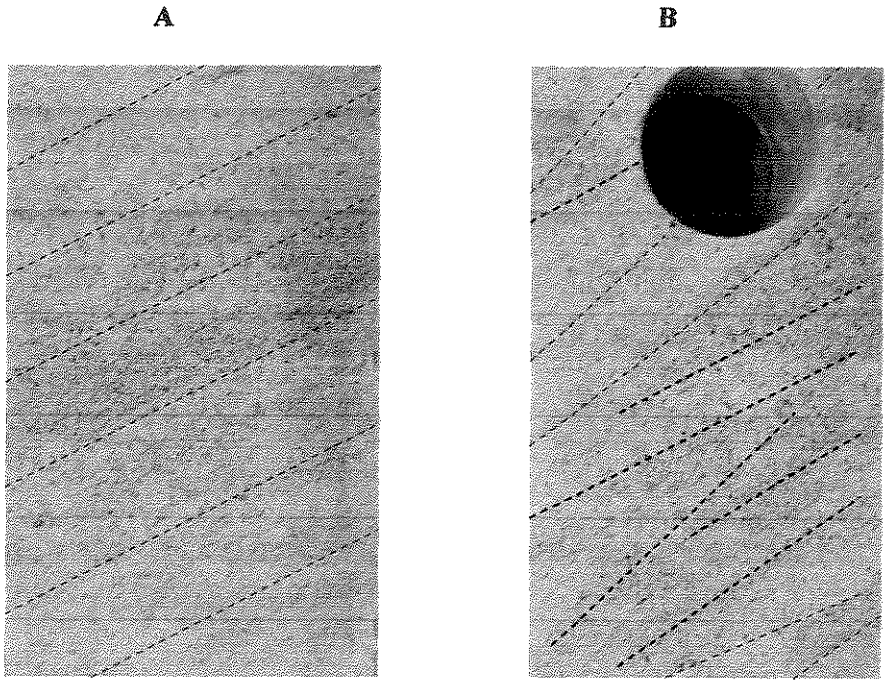

Figure 3 - Parallel bedding (A) and cross bedding sedimentary structures (B) encountered in the core depth interval of 2072.00m-2072.26m and 2072.26m-2072.48m respectively.

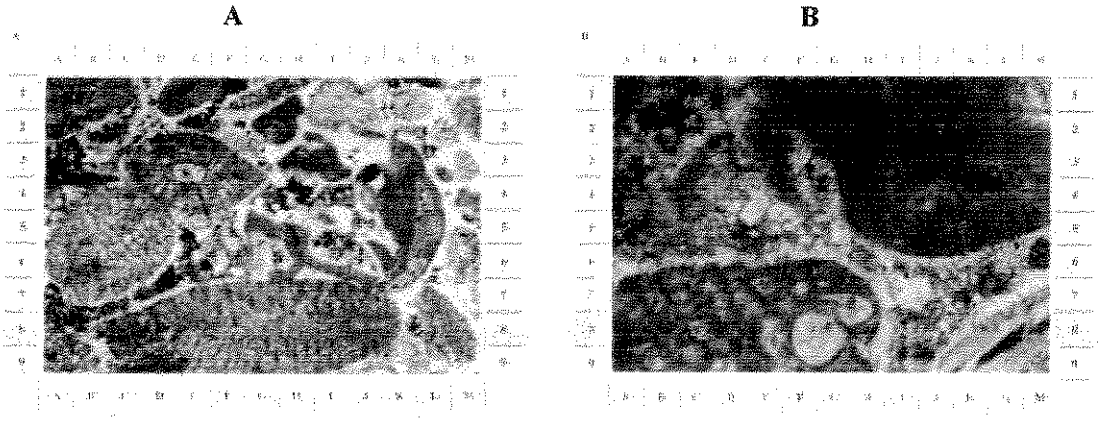

Figure 4 - Petrography analysis showing that this facies mainly comprises of larger foraminifera (C-J,7-9, D-G,3-4, photo:A) and red algae (F-M,1-5, photo:B).

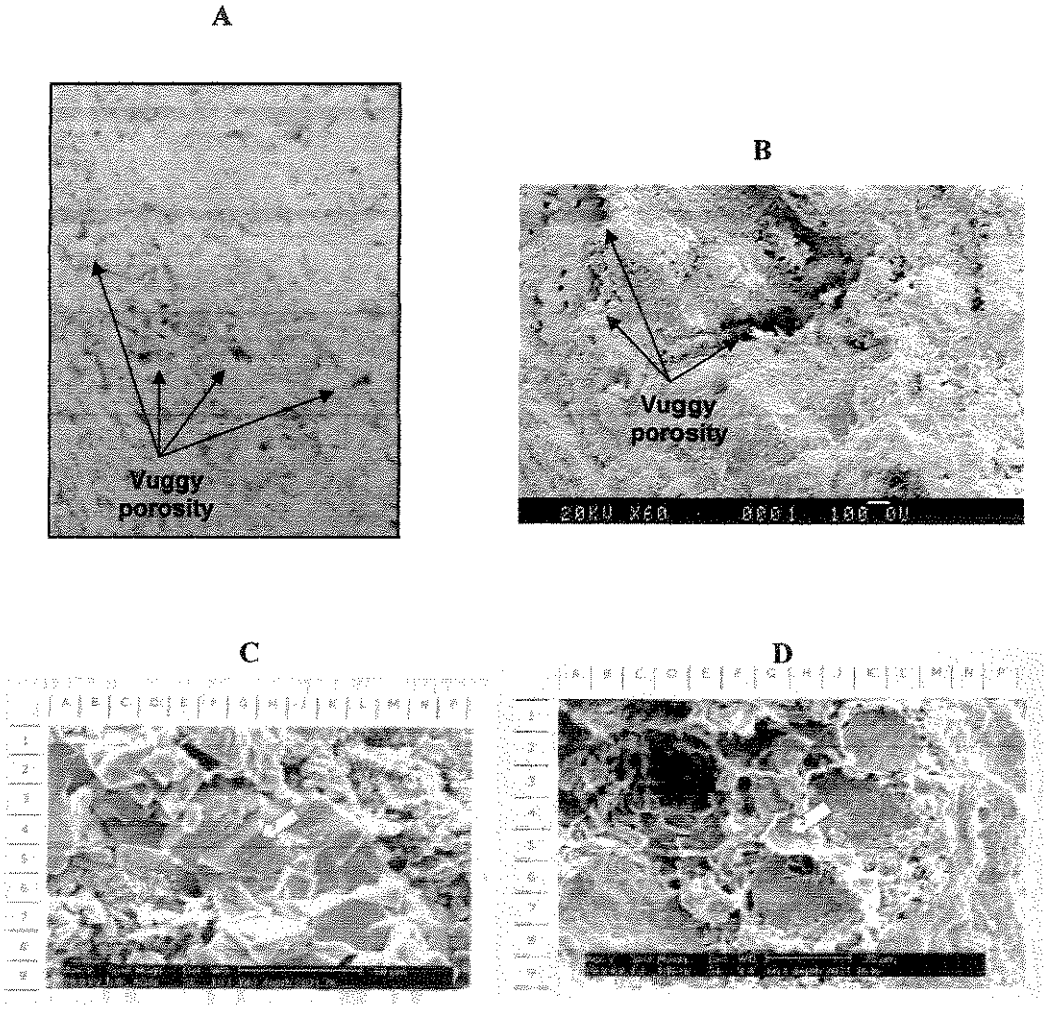

Figure 5 - Vuggy porosity encountered in this rock sample (photo A). General Scanning Electron Microscopy (SEM) shows a *grainstone* has moderate porosity. Pore system is dominated by vuggy porosity (photo B), some intercrystalline and intragranular pore types. Some of vuggy pores are calcite cemented reducing porosity value. Detailed SEM reveals the occurrence of dolomite interpreted by its morphology (arrow 1, photo C) and illite (arrow 2, photo D), this is confirmed by EDX and XRD analysis.

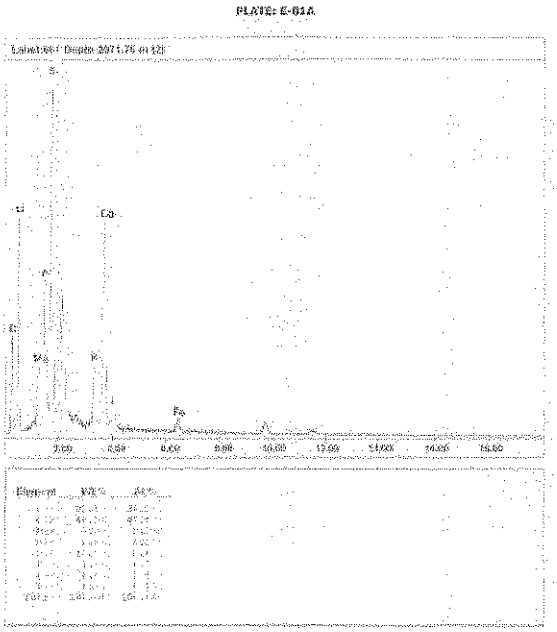

Figure 6 - EDX analysis showing authigenic clay found as illite developed within microporosity.

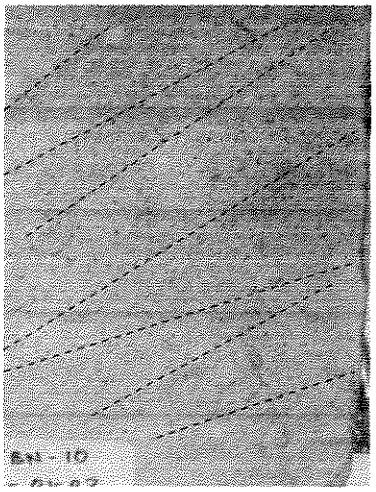

Figure 7 - Cross bedding structure encountered in the Large Foram Packstone to Grainstone Facies.

A B

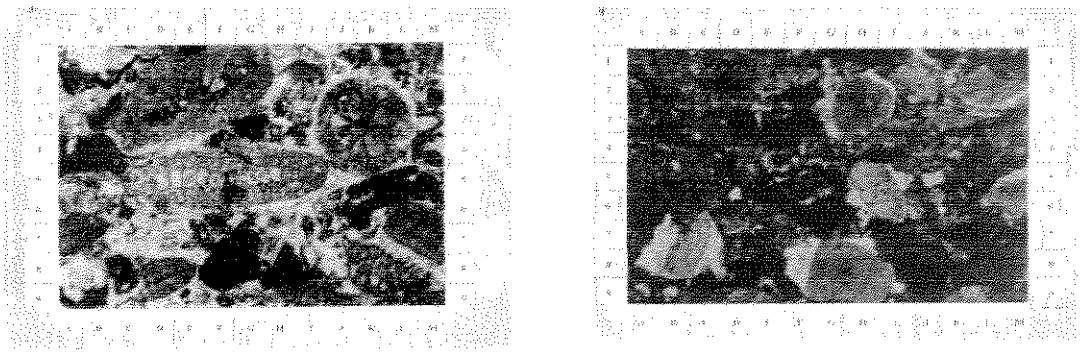

Figure 8 - Detail petrography analysis shows a grainstone mainly consist of large forams (C-I, 5-6; C-G, 2-4; K-L, 8-9: photo-A) and less of red algae (F-G, 8-9; J-M, 6; A-B, 4-5: photo-A), echinoderms (H-I,1-3; H-I, 4-6; G-I, 7-9: photo-B) and small benthonic forams (I,3: photo-A).

Figure 9 - Red Algal Packstone to Floatstone Facies. Minor discontinous thin laminae of detrital clay and carbonaceous materials are present in this facies.

A B

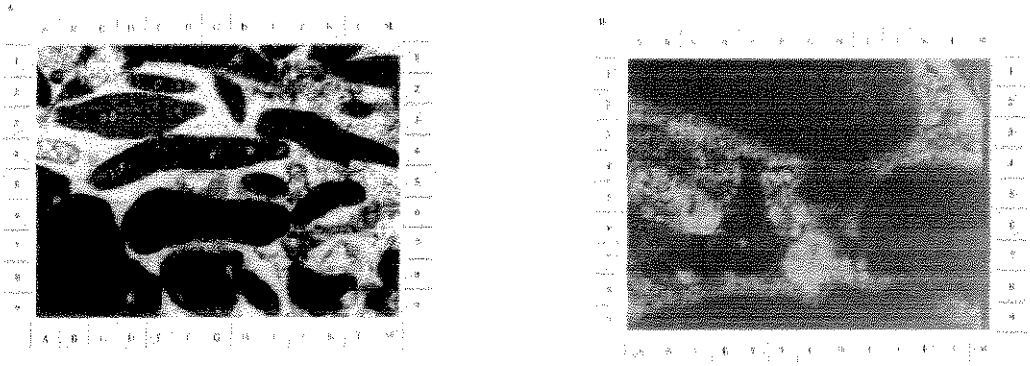

Figure 10 - Detail petrography analysis reveals a grainstone mainly consist of red algae (D-I, 6-7; A-C, 6-9: photo-A) and large forams (A-F, 3-4; C-I, 4-5: photo-A). The porosity type is predominantly mouldic and intergranular pores which are mostly filled by mosaic equant calcite cement and minor of pendant calcite cement type (C-D, 6; C-D, 4; DE, 8: photo-B).

Figure 11 - Red Algal Floatstone to Grainstone Facies. Discontinous thin laminae of detrital clay and carbonaceous materials are present in this facies.

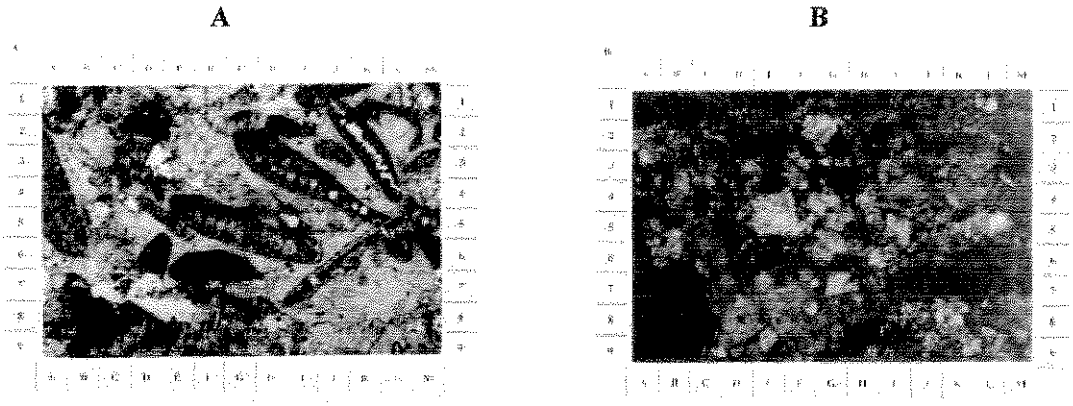

Figure 12 - Detail petrography analysis shows this facies mainly consist of red algae (M,6;C-D,2: photo-A) and large forams (E-I,5-6;A,3-6;E-G,7: photo-A). The porosity type is predominantly intergranular pores which are mostly filled by mosaic calcite cement.

Vp vs Porosity

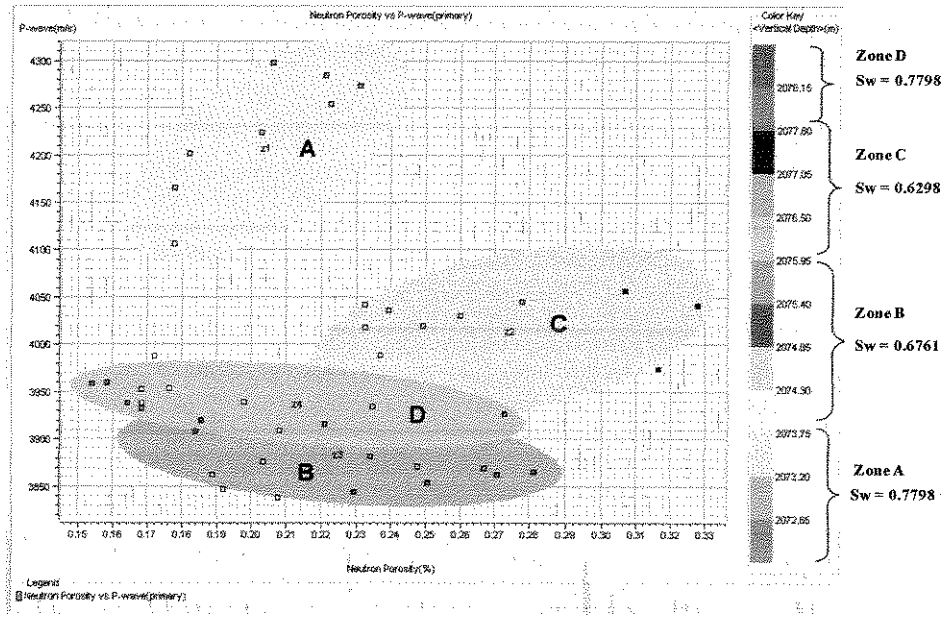

Figure 13 - Porosity (neutron) – compressional wave velocity (Vp) cross plot.

Vp vs Gamma Ray

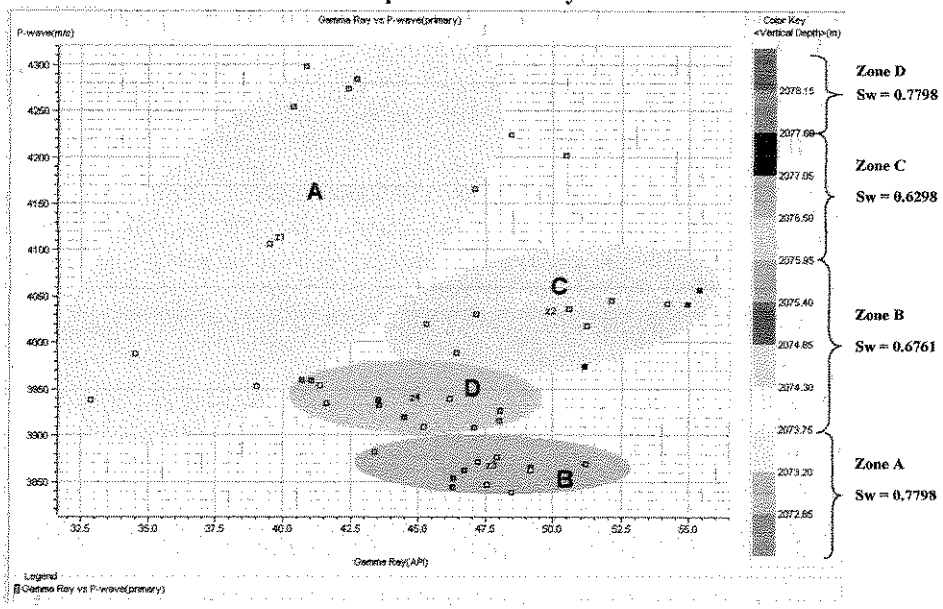

Figure 14 - Gamma Ray – Compressionat Wave Velocity (Vp) Cross Plot.

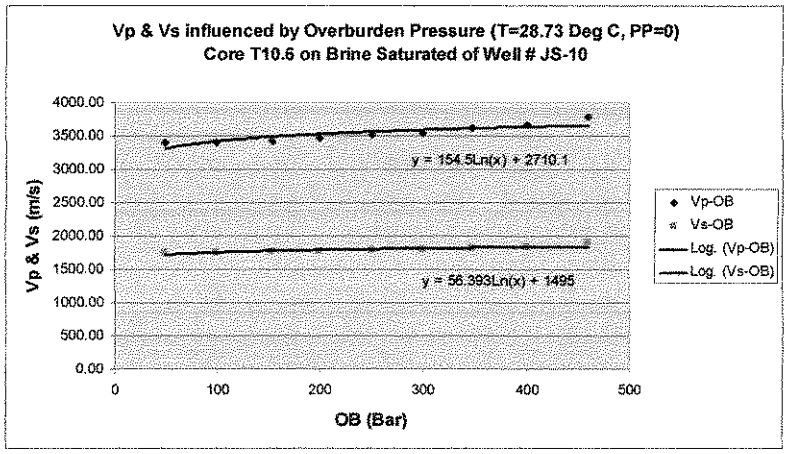

Figure 15 - Vp and Vs influenced by Overburden Pressure (T=28.73 Deg C, PP=0).

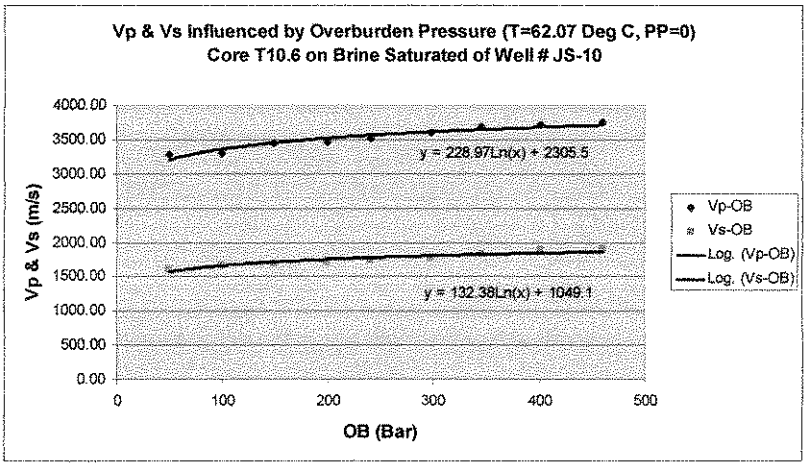

Figure 16 - Vp and Vs influenced by Overburden Pressure (T=62.07 Deg C, PP=0).

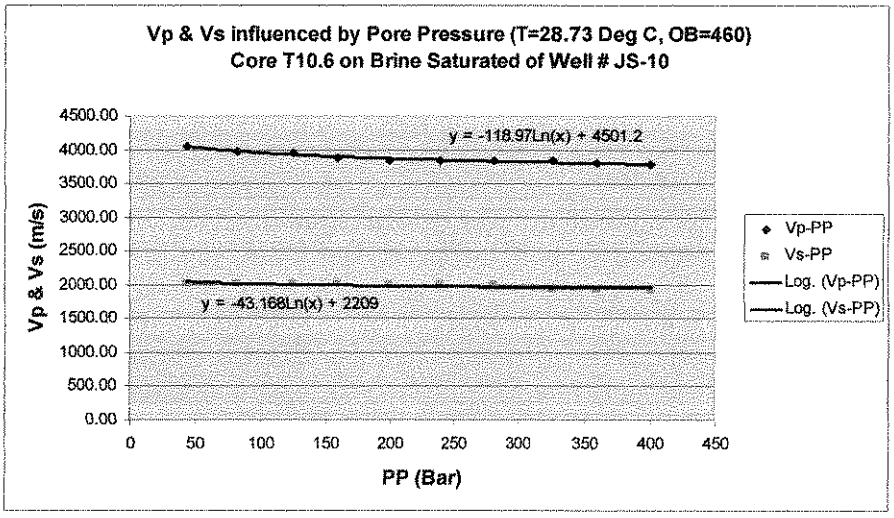

Figure 17 - Vp and Vs influenced by Pore Pressure (T=28.73 Deg C, OB=460).

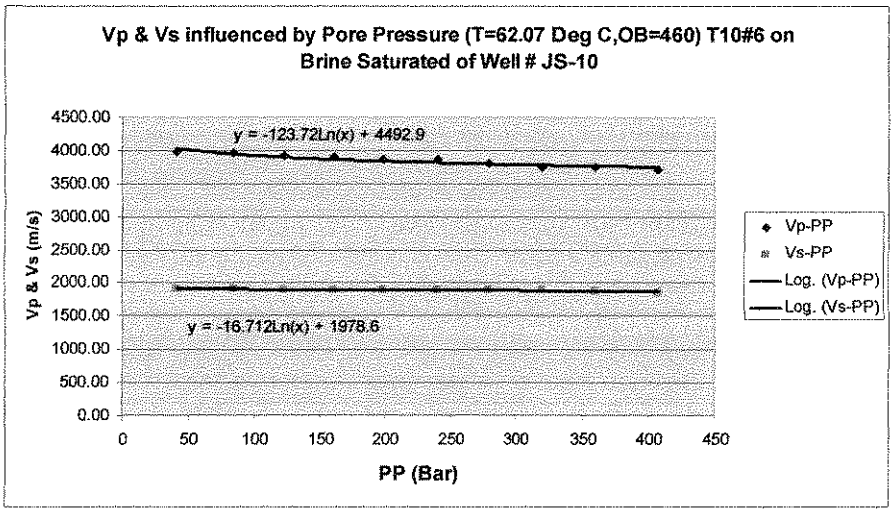

Figure 18 - Vp and Vs influenced by Pore Pressure (T=62.07 Deg C, OB=460).